A conservative flow routing formulation: Déjà vu and the variable-parameter Muskingum method revisited

P. Reggiani *

Deltares, P.O. Box 177, 2600MH Delft, The Netherlands†

E. Todini

Department of Biological, Geological and Environmental Sciences, University of Bologna

Via Zamboni 67, 40126 Bologna, Italy

D. Meißner

Bundesanstalt für Gewässerkunde, Am Mainzer Tor 1, 56068 Koblenz, Germany

*Department of Physical Geography and Climatology, RWTH Aachen University, Aachen, Germany

†Corresponding author, e-mail: paolo.reggiani@deltares.nl, phone: +31-(0)6-51688288

Abstract

A wide range of approaches are used for flow routing in hydrological models. One of the most attractive solutions is the variable-parameter Muskingum (VPM) method. Its majour advantage consists in the fact that *i*) it can be applied to poorly-gauged basins with unknown channel geometries, *ii)* it is fast to execute and *iii)* it adequately captures the most salient features of a dynamic wave also in presence of very mild channel bed slopes, such as the steepening of the rising hydrograph as well as the looped rating curve. In addition, the method offers the possibility to derive average water levels for a reach segment, a quantity which is essential in flow forecasting and flood risk assessment. For reasons of computational economy the method is also appropriate for hydrological applications, in which hydrological and CGM models are coupled and where computational effort becomes an issue. Here we present a review of the VPM approach, set it into perspective from a historical and conceptual point of view and demonstrate its strengths on hand of an application in an operational context.

Keywords: Channel routing, variable-parameter Muskingum, integral formulation, flux closure, mass and momentum conservation.

1 Introduction

The spectrum of channel routing methods in hydrological applications is broad. The options reach from simple linear translation models to a complete dynamic description of channel flow at the other end. The choice usually depends on the scientific background of the modeller and the particular problem at hand. Hydrologist generally opt for conceptual approaches, while people with a channel hydraulics background prefer physically-based solutions, starting out from the full dynamic wave model or simplifications thereof. Examples include the simplification of the dynamic wave model to obtain a hyperbolic differential equation (Price, 1985), or the diffusion wave (DW) analogy formulated as parabolic equation by combining mass and momentum conservation, while neglecting acceleration terms (Hayami 1951, Lighthill and Whitham 1955, Dooge 1973). The DW can be used as linear model with constant parameters for which an integral analytical solution can be found (Hayami 1951, Dooge 1973), or as a linear model with variable parameter values locally linearized in time as in Todini & Bossi (1986). The non-linear version with variable parameters is more complex and needs to be solved numerically. Examples include the work by Cappellaere (1997) and the recent note by Price (2009).

A further simplification of the full dynamic model is the kinematic wave, in which the friction slope is assumed equal to the bed slope. This is possible when the kinetic and the inertial gradients are negligible with respect to the bed and friction slopes. In analogy to the DW, the kinematic model can be formulated with constant or variable parameters, obtaining a linear or non-linear version respectively. The integral form of the kinematic model leads to a linear (Nash 1957, Ostrowski 1992) or non-linear

(Liu & Todini 2004) reservoir equation, for which analytical solutions can be found. However, while reservoir cascades may be appropriate for flow routing within well defined application limits, a more complete dynamic routing becomes indispensable when describing channel flow of large systems also in presence of very mild slopes (in the order of 10^{-4} or milder), where the kinetic and inertial gradients become relevant.

In this context Gąsiorowski and Szymkiewicz (2007) have provided a significant contribution towards the understanding of conservation properties of the non-linear kinematic and DW equations. Their analysis of integral terms demonstrates that by integrating variable-parameter models, whose governing equations hold at the point-scale, over finite time and space domains, mass and momentum cannot be simultaneously conserved while only linear (thus constant parameter) models remain conservative in the integral form. The reason is the non-divergent form of the non-linear governing equation. These considerations are interesting, because the conservation properties of widely used models have rarely been addressed from a purely analytical perspective and hardly any attention has ever been paid to the conservation of momentum. Said conservation properties require an a-priori knowledge on the operational limits of a particular model and for this reason form a central topic of this paper.

A commonly used alternative to the dynamic wave model is the variable-parameter Muskingum (VPM) routing method. Cunge (1969) modified the original fixed-parameter linear approach introduced by McCarthy (1940), which he interpreted as a first-order kinematic approximation of a DW model. He changed it into a non-

linear parabolic model by allowing for variable parameters. These are then defined by imposing a match between physical and numerical diffusion. Todini (2007) revised and generalized the VPM method by delivering an explanation for why the original scheme is not mass-conservative, as repeatedly observed several years earlier (Ponce and Yevjevich, 1978, Tang et al. 1999, Cunge 2001). The principal strength of the VPM approach remains the fact that it can be implemented with comparatively modest input data and does not require detailed channel geometries. The latter are needed by the full dynamic wave model, but are frequently unavailable in practice. Moreover the computational demand is comparatively low, making the approach appealing for representing surface flows in complex land-surface schemes within GCM simulations.

Aim of this paper it to take a fresh look at the VPM method, especially the mass-conservative formulation (MCT) introduced by Todini (2007), by casting it in the light of a conservative integral formulation. Starting from the point-scale conservation for mass and momentum, we integrate these over a channel reach segment. The resulting unknown boundary fluxes need to be closed by combining mass and momentum conservation. From a more modern perspective the method can be envisaged as an endeavour of tackling the closure of hydraulic fluxes at the scale of a hydrologic control volume. As such the approach is a mosaic tile within the larger puzzle of perceiving watershed hydrology as a problem of mass, momentum or energy flux closure across boundaries of scale-independently defined control volumes (Reggiani et al. 1998, 1999). The search for appropriate closure relations for hydrologcic fluxes has been proclaimed a major challenge of hydrology of the 21st century by

Beven (2001, 2006).

The paper is structured as follows: Section 2 revisits the point-scale equations, Section 3 the derivation of the dynamic wave model, Section 4 presents the integral formulation, Section 5 addresses the flux closure and puts the Muskingum method into perspective, Section 6 provides a discussion while Sections 7 and 8 describe an application to a practical study case.

2 Microscale formulation

The conservation equations for a generic thermodynamic property ψ of a fluid at the microscale can be written in tensor notation as follows (Eringen 1980):

$$\frac{\partial(\rho\psi)}{\partial t} + \nabla \cdot (\rho\psi\mathbf{v}) - \nabla \cdot \mathbf{i} - \nabla(\rho f) = 0 \tag{1}$$

where $\mathbf{i}$ is a diffusive flux and f is an external supply of ψ. To obtain microscale mass and momentum equations, ψ, $\mathbf{i}$, and f are replaced by the properties listed in Table 1, where $\mathbf{T} = -p\mathbf{I} + \tau$ is the total stress tensor, p the pressure, $\mathbf{I}$ the identity matrix and τ the viscous stress tensor. For an incompressible fluid the microscale mass and momentum equations become:

$$\nabla \cdot \mathbf{v} = 0 \tag{2}$$

and

$$\rho\frac{\partial \mathbf{v}}{\partial t} + \rho\nabla \cdot (\mathbf{v}\mathbf{v}) - \nabla \cdot \mathbf{T} - \rho\nabla\mathbf{g} = 0 \tag{3}$$

respectively, whereby ψ is set equal to the velocity $\mathbf{v}$, $\mathbf{i}$ to the total stress tensor $\mathbf{T}$ and f to the gravity vector $\mathbf{g}$.

insert Table 1 here

3 Infinitesimal-scale formulation

The dynamic wave model, known as Saint-Venant (SV) equations, is derived by averaging the microscale equations (2) and (3) over a slab of infinitesimal thickness orthogonal to the channel axis. In the averaging process the SV assumptions (Chow 1968) are applied. The resulting 1-D mass conservation equation, which is now infinitesimal along the channel axis and finite-dimension over the cross-section, becomes:

$$\frac{\partial A}{\partial t} + \frac{\partial Q}{\partial x} = 0 \tag{4}$$

with Q the discharge and A the cross-section area at axis point x and time t. Similarly the infinitesimal momentum equation averaged over the slab reads:

$$\frac{\partial Q}{\partial t} + \frac{\partial \left(Q^2/A\right)}{\partial x} + gA(\frac{\partial y}{\partial x} - S_0) + gAS_f \quad = \quad 0 \tag{5}$$

where y is the flow depth, S_0 is the local bed slope and S_f the friction slope. S_f can be related via Manning law to the steady-state discharge Q_0 and the local hydraulic radius. After rearranging corresponding terms, the following expression is obtained:

$$Q = Q_0 \left[1 - \frac{1}{S_0}\frac{\partial y}{\partial x} - \frac{1}{S_0 g A}\frac{\partial \left(Q^2/A\right)}{\partial x} - \frac{1}{S_0 g A}\frac{\partial Q}{\partial t}\right]^{1/2} \tag{6}$$

Eq. (6) highlights, which terms contribute to the local discharge under dynamic conditions by adding correction terms to Q_0. Depending on a particular situation, individual terms between square brackets have higher importance over others, which

become negligible. For instance in the case of a kinematic wave, the surface gradient, as well as the convective and local acceleration become unimportant. In the diffusive wave model the two acceleration terms can be dropped, while the full dynamic wave model requires all acceleration components to be retained. The set of equations (4) and (5) constitutes the dynamic wave model and needs to be solved numerically. Under assumption of negligible inertia and linearisation (Hayami 1951, Lighthill and Whitham 1955, Dooge 1973) or by applying perturbation analysis (Price 1985), (4) and (5) can be merged first into a hyperbolic and then a parabolic infinitesimal-scale equation (infinitesimal along the channel axis and integral over the cross-section) in only Q (or alternatively y), known as diffusive wave (DW) model:

$$\frac{\partial Q}{\partial t} + C(y, \partial y/\partial x)\,\frac{\partial Q}{\partial x} + D(y, \partial y/\partial x)\,\frac{\partial^2 Q}{\partial x^2} = 0 \tag{7}$$

with C the celerity and D the diffusion coefficient, which expresses the wave attenuation, both non-linear functions of y and $\partial y/\partial x$, also replaceable by Q and $\partial Q/\partial x$ (Capellaere 1997). For constant parameters a linear DW is obtained, for which analytical solutions were found by Hayami (1951) through perturbation analysis or by Dooge (1973) on the basis of Laplace transforms. Todini & Bossi (1986) proposed a solution for the locally linearized DW equation with stepwise constant parameters. Unfortunately, the infinitesimal-scale equation has been frequently "streched" over a finite dimension by numerically integrating it in time and space using the so-called "finite difference" approach (Price 2009).

There are two main reasons for avoiding this approach: Firstly, as pointed out by Gasiorowski and Szymkiewicz (2007), equation (7) with variable parameters cannot

be written in divergent form as it has been obtained on the basis of simplifying assumptions, among which the zero-inertia hypothesis. Secondly, by 'stretching' the infinitesimal solution as to represent the average spatial behaviour, one implicitly assumes that the infinitesimal equations, as well as the domain characteristics and their parameters values, are invariable in each point of the spatial integration domain so that one can write:

$$f\left(\overline{y},\overline{Q}|\overline{\theta}\right) \cong \overline{f}_L = \frac{1}{L}\int_L f\left[y(x,t),Q(x,t)|\theta(x,t)\right]dx \tag{8}$$

where $f(\quad)$ represents the partial differential equation and $\theta(\quad)$ the domain characteristics including the parameter values. Unfortunately this is not the case due to the large spatial variation of cross sections and roughness properties in natural rivers combined with the non-linearity of $f(\quad)$, because the expected value of a non-linear function does not equate the function evaluated in its expected values, unless all parameters and related quantities are constant over the integration domain. As integration in time is not that critical because of the reduced size of the time integration step, finite differences can still be used in time after 'averaging' the equations in space, which become ordinary differential equations as a consequence.

4 Finite-dimension scale formulation

In a finite-dimension scale, equation (1) is averaged (integrated) over a control volume, which we define as a channel segment of finite length. Application of Reynolds transport and Gauss theorems allows to convert the volume integral of spatial gra-

dients into fluxes across the external boundary surface A of the control volume:

$$\frac{d}{dt}\int_V \rho\psi dV + \int_A \mathbf{n}\cdot[\rho(\mathbf{v}-\mathbf{w})\psi - \mathbf{i}]dA - \int_V \rho f dV = 0 \tag{9}$$

where $\mathbf{n}$ is the unit normal to A pointing outward, $\mathbf{v}$ is the fluid velocity and $\mathbf{w}$ is the velocity of A. The finite-dimension mass and momentum balance equations (also called global balance laws) are obtained by inserting the corresponding properties ψ, $\mathbf{i}$, and f according to Table (1). For constant mass density and static control volume boundaries where $\mathbf{w} = 0$, the integral formulation of the mass and momentum balance equations reduce to

$$\frac{d}{dt}\int_V dV + \int_A \mathbf{n}\cdot\mathbf{v}dA = 0 \tag{10}$$

and to the vector equation

$$\frac{d}{dt}\int_V \rho\mathbf{v}dV + \int_A \mathbf{n}\cdot[\rho\mathbf{v}\mathbf{v} - \tau]dA + \int_A \mathbf{n}\,pdA = \int_V \rho\mathbf{g}dV \tag{11}$$

respectively. The portion of boundary surface A interested by mass fluxes and pressure forces are the upstream and down-stream cross sections of the reach segment, while the channel bed is interested by shear stresses. We note that (11) needs to be projected along the direction of the channel axis. In light of the analysis performed by Gąsiorowski and Szymkiewicz (2007), the microscale equations stated in conservative form, have been mapped into a global balance law via integration. No additional terms are needed to balance the sum of terms in (10). Appendix A provides the proof that the finite-dimension momentum balance law (11) is also fully conservative.

On the contrary, space-time integration of the infinitesimal-scale diffusive wave equation (7) over a finite reach segment, as when using finite difference approaches, will

always lead to a non-zero residual term which is needed to balance the global rate of change and boundary flux terms of Q, with the exception of the linear case with constant parameters C and D. This is due to the fact that for variable parameters the convective and diffusive flux terms cannot be stated in divergent form, with the consequence that the global mass and momentum conservation will be inevitably affected. The proof is provided in Appendix B. The mass error in (7) depends among others on wave slope $\partial Q/\partial x$ and may well be small for smooth waves. However, as shown on theoretical grounds, the error is structural. We conclude that the integral mass balance in the form (10) is the only valid global conservation law to be used as basis for a mass-conservative Muskingum flow formulation at the finite or reach scale.

5 Muskingum as integral formulation

The principal challenge in an integral formulation consists in closing boundary flux terms. These can for instance be related to independent state variables of the system. Here we focus on the global mass conservation law (10), which can be stated more concisely in terms of the flux I entering the segment through the upstream boundary, the flux O exiting at the downstream end and the lateral inflow Q^L:

$$\frac{dV}{dt} = I - O + Q^L \tag{12}$$

We note that in line with the finite-dimension formulation, the fluxes I and O are defined on the cross-section interface between two reach elements and not at the reach midpoint. This is also the first time that the Muskingum method parameters

is stated explicitly including lateral inflow. McCarthy (1940) observed that the reach segment volume can be approximated linearly as the sum of a prism and a wedge, and can thus be expressed as linear combination of I and O, where the constant k has dimension $[T]$ and ϵ is dimensionless:

$$V = \epsilon k\, I - (1-\epsilon) k\, O \tag{13}$$

from which a linear storage-flux function $O = O(I, V, Q^L)$ can be explicited. Cunge [1969] introduced variable k and ϵ, allowing for a non-linear storage-flux relationship, since known as Muskingum-Cunge (MC) routing. As recently pointed out by Todini (2007) the derivative of (13) must in that case be obtained by considering the coefficients as functions of time, a facet that had been overlooked by Cunge (1969) and successive works (Ponce and Yevjevich 1978, Ponce and Chaganti 1994), but which is essential for ensuring mass conservation and consistency with the steady state. When the parameters are not constant in time, their expression cannot be taken out of the derivative operator and thus (Todini, 2007) the total derivative of storage in presence of variable parameters becomes:

$$\begin{aligned} \frac{dV}{dt} = \frac{d[\epsilon k\, I]}{dt} - \frac{d[(1-\epsilon)kO]}{dt} = \\ \epsilon k \frac{dI}{dt} + I\frac{d[\epsilon k]}{dt} - (1-\epsilon)k\frac{dO}{dt} - O\frac{d[(1-\epsilon)k]}{dt} \end{aligned} \tag{14}$$

By setting (12) equal to (13) and switching to a discrete notation in time, (15) can be restated:

$$\overline{\epsilon k}\, \frac{\Delta I}{\Delta t} + \frac{\Delta[\epsilon k]}{\Delta t}\, \overline{I} - \overline{(1-\epsilon)k}\, \frac{\Delta O}{\Delta t} - \frac{\Delta[(1-\epsilon)k]}{\Delta t}\, \overline{O} = \overline{I} - \overline{O} + \overline{Q}^L \tag{15}$$

where the time-average $\overline{\ \ }$ is defined as $\frac{1}{2}(\ |_{t+\Delta t} + \ |_t)$ and the difference $\Delta = |_{t+\Delta t} - |_t$. After rearranging the expression, the outgoing flux $O_{t+\Delta t}$ can be stated

as non-linear combination of fluxes with variable parameters:

$$O_{t+\Delta t} = C_1\ I_{t+\Delta t} + C_2\ I_t + C_3\ O_t + C_4 \overline{Q}^L \tag{16}$$

A physical interpretation of k and ϵ has been performed first by Cunge (1969) for a segment of length Δx, width B and slope S_0, whereby he set the numerical diffusion (higher order numerical rounding error) in a finite difference mid-point scheme of the kinematic wave model equal to the coefficient of the second-order term in the DW model. Todini (2007) in his revised mass-conservative and steady-state consistent analysis redefined the original $k = \Delta x/c$ with c $[L/T]$ the wave celerity, as $k^* = \Delta x/v$ with v $[L/T]$ the reach velocity and ϵ as

$$\epsilon^* = \frac{1}{2}\left(1 - \frac{qv}{c^2 \Delta x B S_0}\right) \tag{17}$$

where q is a reference discharge, a quantity which can be estimated explicitly (Cunge 1969, Ponce and Yevjevich 1978) or implicitly at the grid nodes using multiple support points (Ponce and Chaganti 1994). The full development of (16) is given in Appendix C.

6 Discussion

Next we analyse the historical perception of the VPM approach from a conceptual perspective. Although the Muskingum solution (16), after integration of the mass balance equation in time, corresponds to the solution of an ordinary differential equation (ODE), frequently in the literature (16) is taken as the solution of a partial differential equation (PDE). Cunge (1969) was the first to draw the parallel between

(16) and a time-centred four-point finite difference form of (7) with $D = 0$, with the aim to find a physical interpretation for the variable parameters. From there onwards the tradition of envisaging the VPM method as a discrete form of the DW model persisted (Ponce and Chaganti 1994, Perumal 1994, Tang et al. 1999, Wang et al. 2006), with the most recent example being the statement by Price (2009) that the mass-conservative variable-parameter method (MCT) proposed by Todini (2007) constitutes the solution of a space and time-centred finite-difference discretization of (7).

In setting the two concepts equal, two things are principally confused: a) the infinitesimal-scale representation of the mass and momentum conservation as in (4)/(5) and b) the integral formulation (10) used by McCarthy (1940) as basis of the Muskingum method. The details are discussed hereunder:

- Any finite difference discretization of (7) used as a approximation of (16), is an infinitesimal-scale formulation (infinitesimal along the channel axis and finite over the cross section) which is "stretched" to the finite length of the reach instead of using an equation resulting from its integration over a finite domain. Due to the non-linearity of the equations the two solutions are different unless the domain is characterised by constant values of the parameters and the flow, as in a channel under uniform flow conditions, a situation which is unlikely to be encountered in natural rivers.

- The finite difference discretized equation for the reach is expressed in terms of water depth and flux gradients, which are *both* evaluated at the reach interfaces. This is a condition which does numerically not guarantee mass balance, as

pointed out by Patankar (1980) and acknowledged by several authors (e.g. Stelling and Duinmeijer 2003) and which led to the staggered grid methods chiefly used in two dimensional problems.

- As shown analytically by Gąsiorowski and Szymkiewicz (2007) (7) does not simultaneously conserve mass and momentum as it is written in a non-divergent form. Consequently any finite difference solution of (7) cannot be conservative either.

- Equation (16) constitutes a discrete form of an ordinary differential equation (ODE), which results from the global balance law (10) formulated directly at the reach scale. The mass exchange across the boundary is expressed as inflow/outflow fluxes, which are defined at the reach segment interfaces, while quantities such as reference discharge q, stage y or cross section area A are expressed as reach-averages.

- By solving for mass fluxes on the interface and calculating remaining quantities at the reach midpoint, the VPM method in the conservative form (MCT) presented by Todini (2007) is equivalent to a staggered-grid scheme, in which fluxes are calculated on the boundary of the computational cell and scalar variables at the cell centre. The advantage of using staggered grids in the interest of an accurate numerical solution has been explained by Patankar (1980) and is manifested in case of fluctuating fields.

- The MCT is mass-conservative because the underlying finite-dimension mass balance is written in conservative form (Appendix A) and the flux closure has been corrected for the time-derivative of the parameter product $k \cdot \epsilon$, as shown

in Section 5. It is also consistent with the steady state, as the Cunge (1969) parameter k, a reach transition time defined as ratio of cell size and wave speed (Section 5), has been replaced by k^*, the ratio of cell size over velocity. This is a natural consequence of the integral formulation, as opposed to the analogy drawn with the infinitesimal-scale DW by Cunge; the concept of celerity is implicit in the DW equation (7) but extraneous to the integral conservation law (10). In the case of a wide rectangular channel $c \approx 5/3\ v$, which highlights the difference in magnitude between the two parameters and the respectively induced error.

- The difference between Price's (2009) finite difference approximation of the DW and Todini's (2007) Muskingum parameters consists in the fact that the former calculates Q as well as q, A and y as solution of a space-time discretized partial differential equation (PDE) all at the interfaces of a predefined computational grid, while the latter calculates Q on the reach segment interfaces and y and A at the mid-point as solution of a non-linear ordinary differential equation (ODE) for a finite volume. It should be noted that Price (2009) integrates the PDE over the finite domain reach exclusively to compare the integral result (Eq.(17) in Price 2009) with Todini's MCT (2007) and then sustains that Todini's result equals the finite difference solution given his Eq. (10). This is however not so.

- While the VPM has been looked upon in the hydraulic literature as an approximate routing method suitable for hydrological application, the MCT has been shown to be fully consistent with first principles. When the diffusive approxi-

mation holds, the MCT version of the VPM is thus equivalent to the solution of the dynamic wave equation, but easily applicable in ungauged basins, where channel geometry information is scarce or unavailable.

7 Application

7.1 Model intercomparison setup

To verify the MCT for a real-world case we applied it to flood propagation in the river Mosel. The Mosel drains a 29.000 sqkm basin and is one of the largest tributaries to the river Rhine. The long-term average flow in the proximity of Koblenz is about 330 m^3/s. Peak discharges of approximately 4200 m^3/s have been recorded, making the Mosel a significant flow contributor to the Rhine. Accurate flow forecasting in the river Mosel is important, and attracts stakeholder interest to compare computational and forecasting performance of non-linear routing methods. A drawback of using the Mosel river system for the present study is the high level of river training, as the Mosel also serves navigation and hydro-electric generation purposes. The engineering works have a severe impact on low flow regimes, but their effect is felt more during low flow periods and gradually disappears during medium to high flows, where the structures are operated in such a way as to allow floods to propagate undisturbed.

8 Simulations

The verification is performed on hand of flow simulations for the 1/1/1996−31/12/2001 period. The lateral inflows were generated using raw forcing data on the REW hydrological model (Reggiani and Rientjes, 2005, 2010). No data assimilation or input correction was applied to the hydrological model to address the input uncertainty, therefore the reproduction of observed flow is not optimal. Main purpose of this exercise it to compare the MCT performance against the dynamic wave solver SOBEK (Stelling and Verwey 2005), which is used for flow forecasting operations by the Federal Institute of Hydrology (BfG) and acts as reference case. The channel geometry for the MCT, mainly the channel width B and the celerity $c = \partial Q/\partial A$ has been determined on the basis of a combination of the at-a-station and downstream hydraulic geometry relationships by Leopold & Maddock (1953) as described in Snell & Sivapalan (1995) and also used by Reggiani et al. (2012) on the Mosel river. The reach segments have been set to al length of 1 km. In SOBEK 455 surveyed high-resolution cross sections were used, about one every 500 m. The computational grid includes 726 nodes over a total model length of 240 km. The Manning roughness is variable with values ranging between 0.022 - 0.025. Figure 1 shows a schematic view of the model setup.

9 Results

Next we present the results consisting of a comparison between the original VPM method, referred to as Muskingum-Cunge (MC) solution, and the mass-conservative

and steady-stated consistent solution (MCT) presented in this paper. In addition we also report the results for the MC and the MCT solutions, in which we apply the Capellaere (1997) slope correction. This correction modifies the bed slope in (17) through multiplication by a factor, which depends of the free surface slope. The latter is approximated as the difference of reach-average water depth over the length of the reach segment. The water depths are estimated from the reach-average discharge through the empirical channel geometry relationships reported in Section 8. The MC version with the Capellaere correction is indicated as MCc and the corrected version of the MCT as MCTc. All four solutions are compared against the dynamic wave solution of the SOBEK model, which we denote as Saint-Venant (SV). The time step in the Muskingum method has been selected safely as 1800s, as longer time steps can potentially lead to a deterioration of the solution. As base case we assign a minimum bed slope of $2.5 \cdot 10^{-4}$, which is imposed as hard minimum value and is in line the minimum slope assigned in the operational SOBEK model of the Mosel. We note that in the case of the MCc and MCTc solution the slope is reduced, if a correction factor smaller than one is calculated, thus effective slope values smaller than $2.5 \cdot 10^{-4}$ are in this case admissible. For the pure reason of analysing the conservation properties of the MC and MCT methods we have also performed simulations with minimum slopes of $1 \cdot 10^{-4}$ and $0.5 \cdot 10^{-4}$ (and thus lower for the MCc and MCTc with the Capellaere correction). For such flat channels the flow is chiefly driven by surface gradients an the solution becomes more akin to that of the parabolic equation.

Figure 2 shows an inter-comparison of all four solutions for a minimum slope of

369 $2.5 \cdot 10^{-4}$ with observations on the same graph at Cochem for a selected triple-peak
370 event which occurred during the 9/12/1999 to 6/1/2000 period. All Muskingum
371 solutions slightly overestimate the maximum peaks, however the rising as well as
372 falling limbs and the peak timing are well captured and in line with the SV solution.
373 We note that for the selected slope the discharge estimates for MC and MCT are
374 quite similar.
375 Figure 3 demonstrates the discrepancy of the storage of the MC approach vs. the
376 storages of the MCT and MCTc solutions. The vertical axis represents the cross sec-
377 tion areas at Cochem over the 9/12/1999 to 6/1/2000 period. The area is calculated
378 as computed reach storage divided by the uniform reach length of 1km and acts as
379 proxy for storage. It is evident that the MC formulation with parameters k and ϵ
380 structurally underestimates reach storage and thus reach-average cross-sections by
381 about 34 % (slope of $2.5 \cdot 10^{-4}$) with respect to the MCT storage formulation (C.5)
382 based on the corrected parameters k^* and ϵ^*. Column 6 in Table 2 summarizes the
383 overall network storage errors for different slope values.
384 The effect of the storage error becomes clear if we evaluate the reach-average mean
385 depth form the cross section. This quantity is needed to draw the looped stage-
386 discharge curves depicted in Figure 4 for the MC and the MCT solutions respectively,
387 which are compared against the curves obtained with the SOBEK model for surveyed
388 sections at Cochem and Trier. We note that the loop is not very pronounced,
389 because the Mosel behaves quasi-kinematic given slopes of $2.5 \cdot 10^{-4}$ and higher.
390 While the empirical cross sections constitute approximations of the actual ones and
391 differences are therefore to be expected, it is clear that the MCT solution reproduces

the curves adequately over the entire flow range. The MC solution on the other hand systematically underestimates the reach-average stage, thus exposing the systematic storage estimation error of the MC vs. the MCT. Figure 5 finally shows for pure demonstration purposes the loops for the (unrealistic) minimum slope of $0.5 \cdot 10^{-4}$ which are clearly more pronounced an one would expect.

Last but not least the reader is reminded that the simulations have been performed over a consecutive period of 6 years, involving multiple peak events. In presence of minimum slopes of $2.5 \cdot 10^{-4}$, both the MC and the MCc loose slightly mass at Cochem with respect to the MCT and MCTc (Column 4 of Table 2). In this context we note that only a minor portion of about 10 % of the total network length used in the model (2101 km) has a minimum slope of $2.5 \cdot 10^{-4}$, while the remaining 90 % are steeper. The overall mass loss remains therefore quite limited when compared against the total volume transited at Cochem (ca. $67.17 \cdot 10^9\, m^3$). This would change however, if the entire network would be flatter. As the slope falls below $2.5 \cdot 10^{-4}$, a situation arises in which the flow is driven essentially by free surface gradients. The mass error for MC and MCc persists, while MCT and MCTc remain fully conservative with a relative error in the order of $1E-16$ (Column 5 in Table 2). The relative mass error is evaluated as:

$$\text{rel. mass error } (\%) = \frac{V_0 + \sum_{i=1}^{n} (\overline{I}_i - \overline{O}_i + \overline{Q}_i^L)\Delta T - V_T}{\sum_{i=1}^{n} \overline{O}_i \Delta T} \times 100 \qquad (18)$$

where ΔT is the simulation timestep, $T = n \cdot \Delta T$ is the 6-year simulation period, V_0 and V_T are the total initial and final volume stored in the network, $(\overline{I}_i + \overline{Q}_i^L)$

is the total network inflow (at upstream network head nodes and lateral) averaged over the timestep i and $\overline{O}_i$ is the basin outflow at Cochem, also averaged over the timestep.

As a concluding remark we observe that the mass loss for the MC/MCc becomes much more apparent when using a straight channel with inflow concentrated at the upper end. In a natural dendritic system such as the Mosel, where a) the inflow is distributed more or less uniformly and b) the slope is in the order of 10^{-3} for a large part of the network, the loss is more obfuscated, but is nevertheless present on the theoretical grounds explained in this paper.

insert Table 2 here

10 Summary and conclusions

The paper discusses the corrected VPM method in the mass-conservative and steady-state consistent version (MCT) introduced by Todini (2007) from a novel perspective. The method is cast into the form of a finite-dimension integral formulation. The principal points of the analysis can be summarized as follows:

- The paper proves that on the basis of an integral formulation the MCT is indeed mass and momentum conservative on theoretical grounds. This is in contrast to the non-linear diffusive wave (DW) equation, which has been shown not to be mass and momentum conservative by Gąsiorowski and Szymkiewicz (2007).
- The finite difference discretisation of the non-linear DW wave model is gener-

ally used to derive the parameters of the VPM method by direct comparison and interpretation. Due to the non-conservative form of the non-linear DW model, these derived VPM formulations are inherently non-conservative, as also repeatedly confirmed in the literature (e.g. Cunge 2001).

- The MCT is based on a finite-dimension mass conservation equation for which boundary fluxes are closed by non-linear storage-flux relationships. The mass fluxes are evaluated at the segment interfaces (upstream and downstream boundaries) in line with the integral formulation, while scalar quantities such as the reference discharge, cross-section area and stage are averages evaluated at the reach centre as for staggered-grid solutions.

- The paper is concluded with a practical application of a six-year continuous flow simulation for the river Mosel. The VPM method in its original form (Cunge 1969) is compared against the MCT (Todini 2007) and the results of the dynamic wave solver SOBEK (Stelling and Duinmeijer 2003).

- While flood routing is performed satisfactorily by all methods, the looped stage-discharge relationships and the area-time plots clearly show the non-conservative behaviour of the original VPM method in terms of systematic underestimation of the stage. Because the stage is a crucial parameter in evaluating flood risk during forecasting operations, only the mass corrected and steady-stage-consistent MCT method can be reliably used for this purpose.

11 Acknowledgements

We acknowledge the E-OBS dataset from the EU-FP6 project ENSEMBLES and the data providers in the ECA&D project. We also acknowledge the International Commission for the River Rhine (CHR) for providing the digital terrain model for the River Mosel basin.

12 References

Beven, K.(2001), How far can we go in Hydrological Modelling, *Hydrol. Earth Sys. Sci*, 5(1), 1-12.

Beven, K. (2006), Searching for the Holy Grail of scientific hydrology: $Qt = (S, R, t)A$ as closure, *Hydrol. Earth Syst. Sci.*, 10, 609-618, doi:10.5194/hess-10-609-2006.

Cappelaere, B. (1997), Accurate Diffusive Wave Routing, *J. Hydraulic Eng.*, ASCE, 123(3),174-181.

Chow, V.T. (1968), Handbook of Hydrology. MCGraw Hill, New York, NY.

Cunge, J.A. (1969), On the subject of a flood propagation computation method (Muskingum Method), *J. Hydr. Res.*, 7(2) 205-230.

Cunge, J.A. (2001), Volume conservation in variable parameter Muskingum-Cunge

method - Discussion, *J. Hydraulic Eng.*, ASCE, 127(3), 239-239.

Dooge, J.C.I. (1973), Linear Theory of Hydrologic Systems, USDA Tech. Bull 1468, U.S. Department of Agriculture, Washington DC.

Eringen, A. C. (1980), Mechanics of Continua, R. E. Krieger Pub. Co..

Gąsiorowski, D. and R. Szymkiewicz (2007), Mass and momentum conservation in the simplified flood routing models, *J. Hydrol.*, 346, 51-58.

Hayami, S. (1951), On the propagation of flood waves, Bulletin no. 1, Disaster Prevention Research Institute, Kyoto University, Japan.

Lighthill, M.J. and Whitham, G.B. (1955), On kinematic waves, I Flood movement in long rivers, *Proc. Roy. Soc. Lon.*, 229A.

Liu, Z., and E. Todini (2004), Assessing the TOPKAPI nonlinear reservoir cascade approximation by means of a characteristic lines solution, *Hydrol. Processes*, 19(10), 1983-2006.

Leopold, L. B., and Maddock, T. Jr. (1953), The Hydraulic Geometry of Stream Channels and some Physiographic Implications, U.S. Geological Survey Professional Paper 252, 56 pp.

497

498 McCarthy, G.T. (1940), Flood Routing, Chap. V "Flood Control", The Engineer
499 School, Fort Belvoir, Virginia, pp. 127-147.

500

501 Nash, J.E. (1957), The form of the instantaneous unit hydrograph, IUGG General
502 Assembly of Toronto, Vol III, IAHS Publ., 114-121.

503

504 Ostrowski, M. (1992), A universal module for the simulation of hydrological pro-
505 cesses, *Wasser und Boden*, Issue 11, pp. 755-760 (in German).

506

507 Patankar, S.V. (1980), Numerical Heat Transfer and Fluid Flow. Hemisphere Pub-
508 lishing Corporation, New York, 197 pp..

509

510 Perumal, M. (1992), Hydrodynamic derivation of a variable parameter Muskingum
511 method, *Hydrol. Sci J.*, 39(5), 431-442.

512

513 Ponce, V. M. and Yevjevich (1978), V.: Muskingum-Cunge method with variable
514 parameters, J. Hydraulic Division, ASCE, 104(12),1663-1667.

515

516 Ponce, V. M. and Chaganti, P. V. (1994), VPM-Cunge revisited, J. Hydrol, 162(3-4),
517 433-439.

518

519 Price, R. K. (1985), Chapter 4: Flood Routing in Rivers, Developments in Hydraulic

Engineering. P. Novak ed., Elsevier Applied Science Publishers, London, 129-174.

Reggiani, P., M. Sivapalan and S.M. Hassanizadeh (1998), A unifying framework of watershed thermodynamics: 1 Balance equations for mass, momentum, energy and entropy and the second law of thermodynamics. *Adv. Water Resour.*, 22(4), 367-398.

Reggiani, P., M. Sivapalan and S.M. Hassanizadeh (1999), A unifying framework of watershed thermodynamics: 2 Constitutive relationships. *Adv. Water Resour.*, 23(1), 15-39.

Reggiani, P. and T.H.M. Rientjes (2005), Internal Flux Parameterisation in the Representative Elementary Watershed (REW) approach: application to a natural basin. *Water Resour. Res.*, 41, W04013, doi:10.1029/2004WR003693.

Reggiani, P. and T. H. M. Rientjes (2010), Closing horizontal groundwater fluxes with pipe network analysis: An application of the REW approach to an aquifer, *Env. Modelling and Software*, DOI:10.1016/j.envsoft.2010.04.019.

Reggiani, P., E. Todini, C. Mazzetti and D. Meißner (2012), An analytical solution of the kinematic wave equation for channel routing, *Hydrology Research* (submitted).

Snell, J. and M Sivapalan (1995), Application of the meta-channel concept: Construction of the meta-channel hydraulic geometry for a natural channel, *Hydrol.*

543 *Proc.*, 9, 485-495.

544

545 Stelling, G. S. and S. P. A. Duinmeijer (2003), A staggered conservative scheme for
546 every Froude number in rapidly varied shallow water flows, *Int. J. Numer. Meth.*
547 *Fluids*, 43, 1329-1354.

548

549 Stelling, G. S and A. Verwey (2005), Numerical Flood Simulation, in Encyclopedia
550 of Hydrological Sciences, John Wiley & Sons Ltd.

551

552 Tang, X., D. W. Knight, and P. G. Samuels: Volume conservation in the Variable
553 Parameter Muskingum-Cunge Method, J. Hydraulic Eng. (ASCE), 125(6), 610-620,
554 1999.

555

556 Todini, E. (2007), A mass conservative and water storage consistent variable pa-
557 rameter Muskingum-Cunge approach, *Hydrol. Earth Syst. Sci.*, 11, 1645-1659,
558 doi:10.5194/hess-11-1645-2007.

559

560 Todini, E. and A. Bossi (1986), PAB (Parabolic and Backwater) an unconditionally
561 stable flood routing scheme particularly suited for real time forecasting and control,
562 *(J. of Hydraul. Res.*, 24(5), 405-424.

563

564 Wang, G. T., Ch. Yao, C. Okoren , and S. Chen (2006), 4-point FDF of Muskingum
565 method based on the St. Venant equations, *J. Hydrol.*, 324, 339-349.

```
566
```

13 Table and Figure Captions

Table 1: Summary of thermodynamic properties in the conservation equation.

Table 2: Mass balance analysis, Cochem, 1996-2001.

Figure 1: Interface between the REW hydrological model and SOBEK.

Figure 2: Discharge values for the 9/12/1999 to 6/1/2000 event at Cochem for SOBEK, the MC and the MCT/MCTc solutions.

Figure 3: Reach-average cross section areas for the 9/12/1999 to 6/1/2000 event at Cochem for SOBEK, the MC and the MCT solutions. The cross section areas serve as proxy for the reach storage.

Figure 4: Looped stage-discharge curves at Cochem and Trier for SOBEK, the MC and the MCT solutions, minimum slope $2.5 \cdot 10^{-4}$.

Figure 5: Looped stage-discharge curves at Cochem and Trier for the MC and the MCT solutions, minimum slope $0.5 \cdot 10^{-4}$.

A Appendix A

The proof for the conservative form of the finite-dimension momentum balance (11) is provided by first splitting the velocity $\mathbf{v}$ into an average velocity and a fluctuation term, which is statistically stationary with zero mean and constant variance:

$$\mathbf{v} = \overline{\mathbf{v}} + \widetilde{\mathbf{v}} \tag{A.1}$$

After substitution into (11) under assumption of constant mass density and application of averaging theory (Gray et al. 1993) one obtains:

$$\frac{d}{dt}\int_V \mathbf{v} dV + (A_{ex} - A_{in})\ \overline{\mathbf{v}}\overline{\mathbf{v}} + \int_A \mathbf{n}\cdot[\overline{\widetilde{\mathbf{v}}\widetilde{\mathbf{v}}} - \frac{\tau}{\rho}]dA + \int_A \mathbf{n}\,\frac{p}{\rho}dA = \int_V \mathbf{g} dV \tag{A.2}$$

whereby the Reynolds stresses $\overline{\widetilde{\mathbf{v}}\widetilde{\mathbf{v}}}$ are added to the viscous ones in a single term. After projection along the channel axis and considering that the tangential viscous stresses act only the bed surface, the vector equation is restated in scalar form:

$$\Delta x \frac{d}{dt}\left(v\ \overline{A}\right) + (A_{ex} - A_{in})\ \left(v^2 + \frac{p}{\rho}\right) + \frac{\Delta x\ P_w}{\rho}\tau_b = g\ S_0\ \overline{A}\Delta x \tag{A.3}$$

As common in open channel flow the shear stress τ_b is expressed as a square function of the average velocity:

$$\tau_b = \frac{\rho\, g}{\overline{R}_H^{1/3}} n^2\ v^2 \tag{A.4}$$

with $\overline{R}_H$ the reach-average wetted perimeter. For uniform flow $A_{ex} = A_{in}$ and (A.3) collapes to Mannings formula. In the non-uniform flow case it is easy to show that no additional non-zero terms are needed to balance (A.2) and therefore the finite-scale momentum formulation for a reach is fully conservative.

B Appendix B

A mathematical proof that the variable parameter DW equation in the form proposed by Cappellaere (1997) is non-conservative is obtained by transforming the infinitesimal-scale parabolic equation (7) into a finite-dimension one through integration over a reach segment of length L (Gąsiorowski and Szymkiewicz, 2007):

$$\frac{\partial}{\partial t}\int_L Q dx + \int_L C\,\frac{\partial Q}{\partial x}dx + \int_L D\,\frac{\partial^2 Q}{\partial x^2}dx = 0 \tag{B.1}$$

By exploiting the chain rule of differentiation (B.1) can be restated:

$$\frac{\partial}{\partial t}\int_L Q dx + \int_L \frac{\partial (C\,Q)}{\partial x}dx + \int_L \frac{\partial}{\partial x}\left(D\,\frac{\partial Q}{\partial x}\right)dx = \int_L \left[Q\frac{\partial C}{\partial x} + \frac{\partial Q}{\partial x}\frac{\partial D}{\partial x}\right]dx \tag{B.2}$$

Thanks to Gauss's theorem the second and third term are converted respectively into convective and diffuse fluxes across the cross-section area A at the reaches ends:

$$\frac{\partial}{\partial t}\int_L Q dx + \left[C\,Q + D\,\frac{\partial Q}{\partial x}\right]_A = \int_L \left[Q\frac{\partial C}{\partial x} + \frac{\partial Q}{\partial x}\frac{\partial D}{\partial x}\right]dx \tag{B.3}$$

For a linear DW C and D are constants and the r.h.s term is zero, yielding a global balance law for Q. For variable C and D the integral yields a non-zero residual:

$$R = -\int_L \left[Q\frac{\partial C}{\partial x} + \frac{\partial Q}{\partial x}\frac{\partial D}{\partial x}\right]dx \neq 0 \tag{B.4}$$

proving that the non-linear version of (7) is non-conservative because it cannot be cast into a divergent form. For instance in the case of a wide rectangular channel of width B (i.e. $B \gg y$) and an energy line which is parallel to the channel bed (i.e. $\partial y/\partial x \approx 0$), $C(Q)$ becomes the kinematic wave velocity, thus C and D can be expressed as functions of Q only (Chow, 1969):

$$C = 1/\left(m\,\alpha\,Q^{m-1}\right); \qquad D = Q/\left(2BS_0\right) \tag{B.5}$$

where:

$$\alpha = \left(n \, P_w^{2/3} S_0^{-1/2} \right)^m \tag{B.6}$$

with $m = 3/5$, P_w the wetted perimeter and n the Manning roughness. It is easy to show that (B.4) is always non-zero for non-zero Q and $\partial Q/\partial x$. By equivalence of the DW equation as reported by Cappellaere (1997) with the one in the form provided by Price (2009), the latter is not conservative either.

C Appendix C

The mass-conservative and steady-state consistent VPM method presented by Todini (2007) extended to include lateral inflow Q^L $[L^3/T]$ is recapitulated. The outflow $O_{t+\Delta t}$ from a reach segment of length the reach of length Δx is given by a linear combination of variable coefficients and the inflow and outflow at time t and $t + \Delta t$:

$$O_{t+\Delta t} = C_1 \, I_{t+\Delta t} + C_2 \, I_t + C_3 \, O_t + C_4 \, \overline{Q^L} \tag{C.1}$$

with $\overline{Q^L} = \frac{1}{2}\left(Q^L_{t+\Delta t} - Q^L_t\right)$. The coefficients expressed in terms of corrected Courant C^* and Reynolds D^* numbers are given by the following expressions:

$$\begin{aligned} C1 &= \frac{-1 + C^*_{t+\Delta t} + D^*_{t+\Delta t}}{1 + C^*_{t+\Delta t} + D^*_{t+\Delta t}} \\ C2 &= \frac{1 + C^*_t - D^*_t}{1 + C^*_{t+\Delta t} + D^*_{t+\Delta t}} \cdot \frac{C^*_{t+\Delta t}}{C^*_t} \\ C3 &= \frac{1 - C^*_t + D^*_t}{1 + C^*_{t+\Delta t} + D^*_{t+\Delta t}} \cdot \frac{C^*_{t+\Delta t}}{C^*_t} \\ C4 &= \frac{2C^*_{t+\Delta t}}{1 + C^*_{t+\Delta t} + D^*_{t+\Delta t}} \end{aligned} \tag{C.2}$$

with

$$C^*_t = \frac{c_t}{\beta_t} \cdot \frac{\Delta t}{\Delta x}; \qquad C^*_{t+\Delta t} = \frac{c_{t+\Delta t}}{\beta_{t+\Delta t}} \cdot \frac{\Delta t}{\Delta x} \tag{C.3}$$

$$D^*_t = \frac{q_t}{\beta_t B S_0 c_t \Delta x}; \qquad D^*_{t+\Delta t} = \frac{q_{t+\Delta t}}{\beta_{t+\Delta t} B S_0 c_{t+\Delta t} \Delta x} \tag{C.4}$$

where c is the wave celerity and $\beta = \overline{A}\ c/q$ a dimensionless correcting factor with $\overline{A}$ the reach-average cross sectional area calculated from the reach storage V as $\overline{A} = V/\Delta x$. From the shape of the cross section the reach-average stage can be evaluated as $y = y(\overline{A})$. The quantity q is the reach reference discharge, which is approximated using an iterative procedure with two or three support points. All quantities must be evaluated at times t and $t + \Delta t$, respectively. The corrected mass-conservative expression for the reach segment storage is:

$$V_{t+\Delta t} = \frac{(1 - D^*_{t+\Delta t})\Delta t}{2C^*_{t+\Delta t}}\ I_{t+\Delta t}\ +\ \frac{(1 + D^*_{t+\Delta t})\Delta t}{2C^*_{t+\Delta t}}\ O_{t+\Delta t} \tag{C.5}$$

Property	ψ	$\mathbf{i}$	f
Mass conservation	1	0	0
Momentum conservation	$\mathbf{v}$	$\mathbf{T}$	$\mathbf{g}$

Table 1: Summary of thermodynamic properties in the conservation equation

case	characteristics	min. slope	cum. outflow (mm)	rel. mass error (%) Eq. (18)	mass error (%) Eq. (13), (C.5)
observed	measured discharge	N/A	$2.33E+03$	N/A	N/A
SV	726 nodes, $\Delta t = 1hr$	$2.5 \cdot 10^{-4}$	$2.40250E+03$	$1E-16$	N/A
MC	$\Delta x = 1km$, $\Delta t = 1800s$	$2.5 \cdot 10^{-4}$	$2.40052E+3$	0.087	33.83
		$1.0 \cdot 10^{-4}$	$2.40061E+3$	0.082	33.97
		$0.5 \cdot 10^{-4}$	$2.40070E+3$	0.077	33.81
MCc	$\Delta x = 1km$, $\Delta t = 1800s$	$2.5 \cdot 10^{-4}$	$2.40051E+3$	0.088	33.82
		$1.0 \cdot 10^{-4}$	$2.40050E+3$	0.088	33.66
		$0.5 \cdot 10^{-4}$	$2.40031E+3$	0.097	33.81
MCT	$\Delta x = 1km$, $\Delta t = 1800s$	$2.5 \cdot 10^{-4}$	$2.40254E+3$	$1E-17$	0.00
		$1.0 \cdot 10^{-4}$	$2.40253E+3$	$1E-16$	0.00
		$0.5 \cdot 10^{-4}$	$2.40252E+3$	$1E-16$	0.00
MCTc	$\Delta x = 1km$, $\Delta t = 1800s$	$2.5 \cdot 10^{-4}$	$2.40254E+3$	$1E-16$	0.00
		$1.0 \cdot 10^{-4}$	$2.40252E+3$	$1E-16$	0.00
		$0.5 \cdot 10^{-4}$	$2.40251E+3$	$1E-15$	0.00

Table 2: Mass balance analysis, Cochem, 1996-2001.

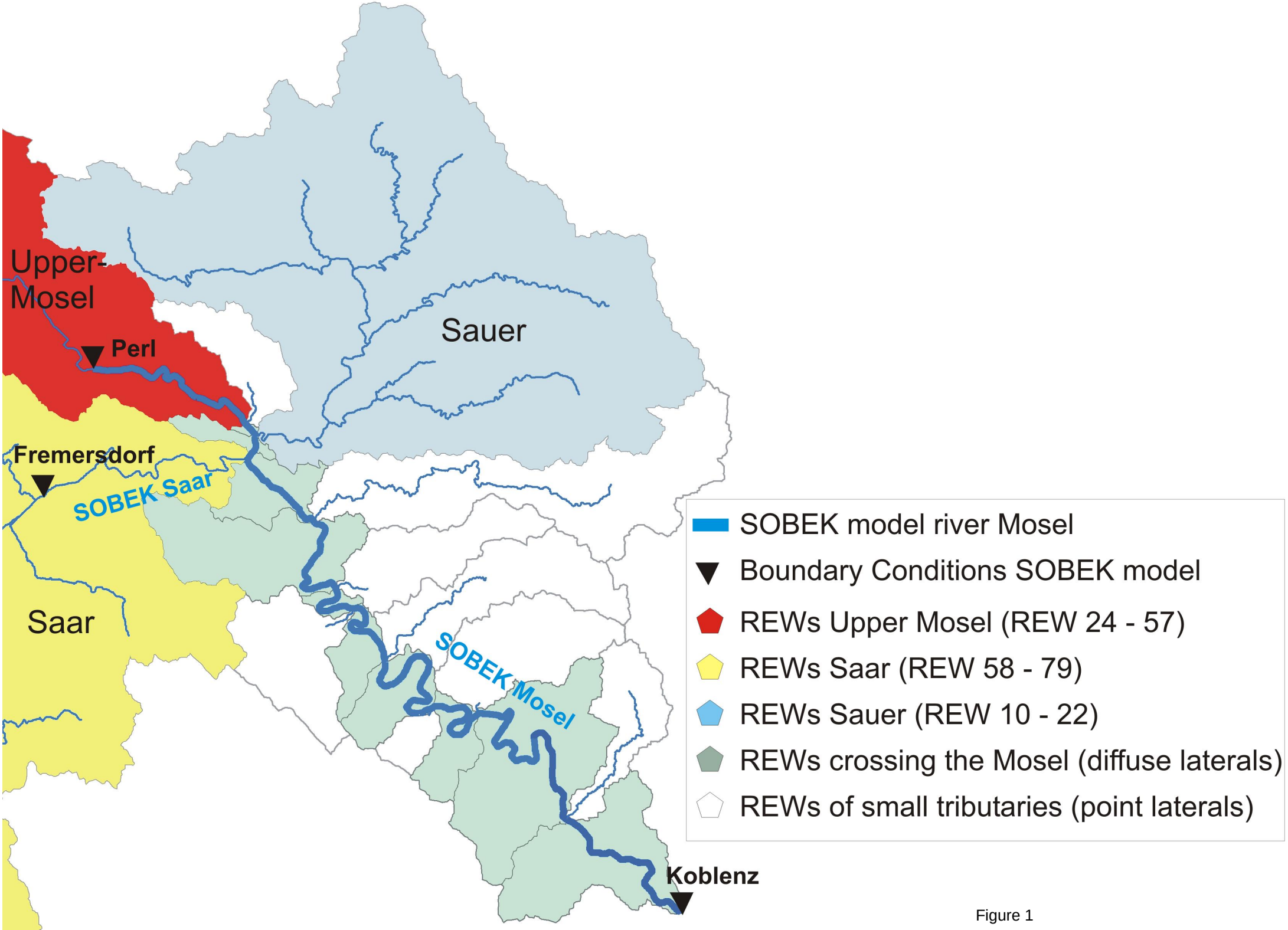
Upper-
Mosel
Perl
Sauer
Fremersdorf
SOBEK Saar
Saar
SOBEK Mosel
Koblenz
SOBEK model river Mosel
Boundary Conditions SOBEK model
REWs Upper Mosel (REW 24 - 57)
REWs Saar (REW 58 - 79)
REWs Sauer (REW 10 - 22)
REWs crossing the Mosel (diffuse laterals)
REWs of small tributaries (point laterals)

Figure 1

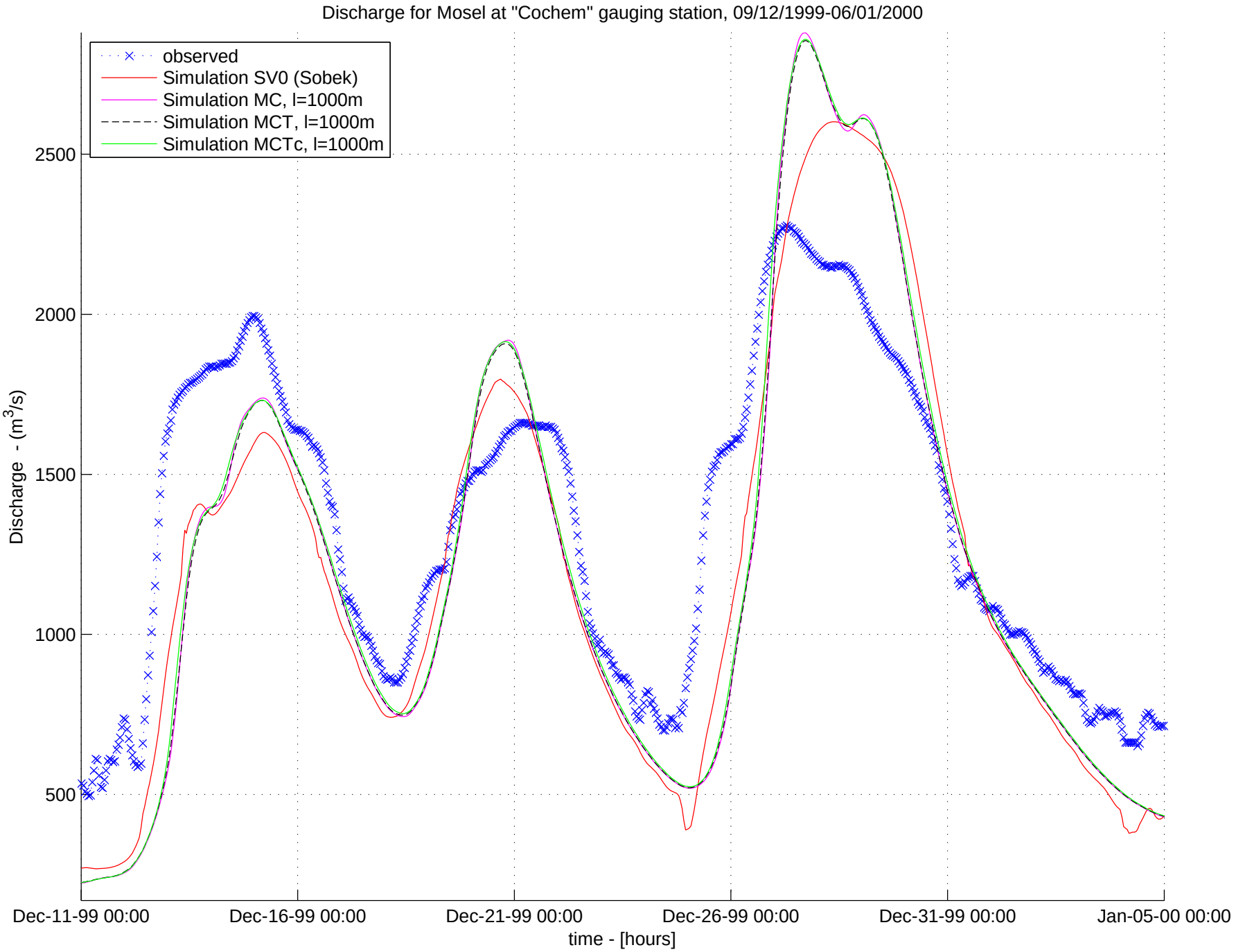
Discharge for Mosel at "Cochem" gauging station, 09/12/1999-06/01/2000
observed
Simulation SV0 (Sobek)
Simulation MC, l=1000m
Simulation MCT, l=1000m
Simulation MCTc, l=1000m
2500
2000
1500
1000
500
Discharge - (m3/s)
Dec-11-99 00:00
Dec-16-99 00:00
Dec-21-99 00:00
Dec-26-99 00:00
Dec-31-99 00:00
Jan-05-00 00:00
time - [hours]

Figure 2

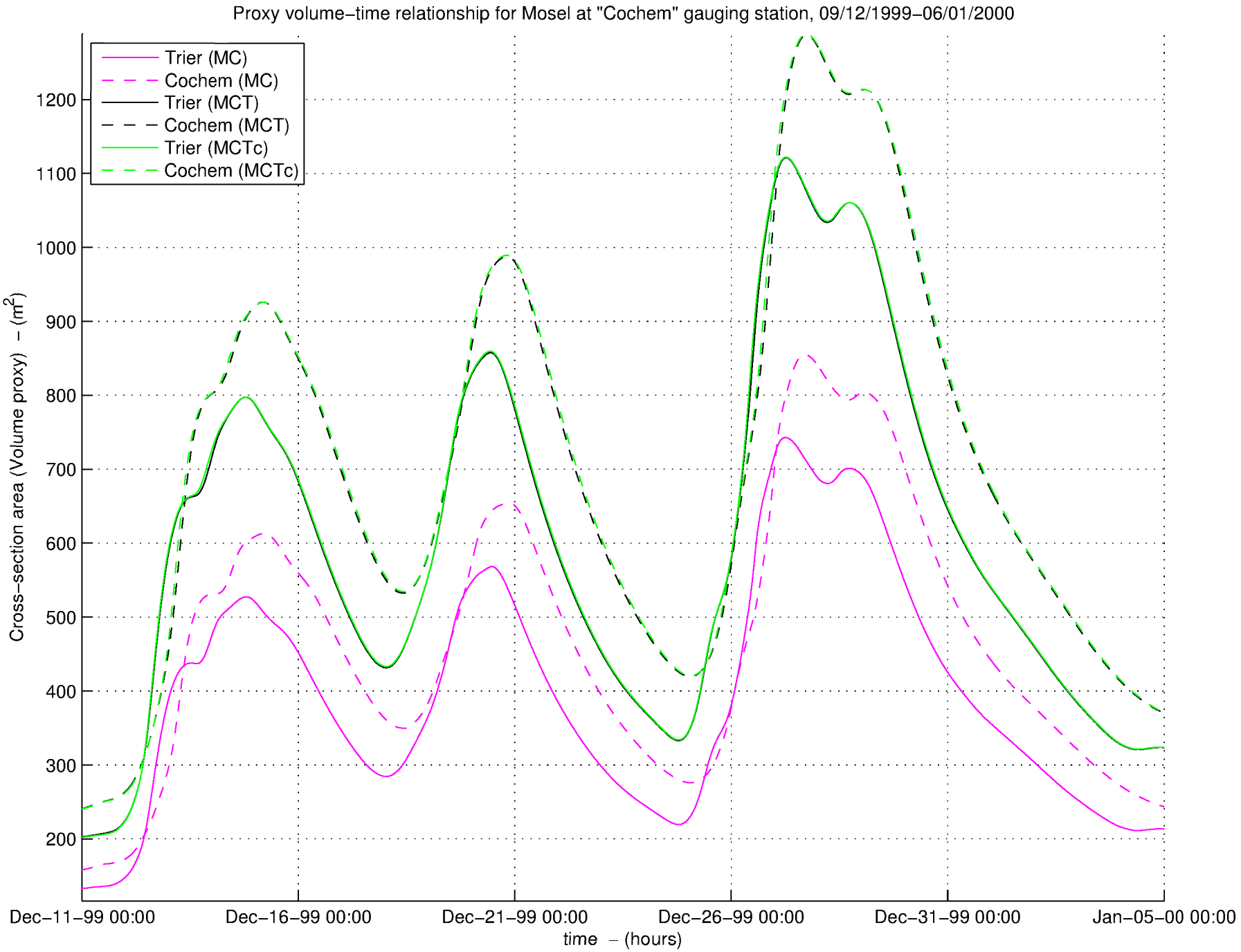
Proxy volume–time relationship for Mosel at "Cochem" gauging station, 09/12/1999–06/01/2000
Trier (MC)
Cochem (MC)
Trier (MCT)
Cochem (MCT)
Trier (MCTc)
Cochem (MCTc)
Cross–section area (Volume proxy) – (m2)
1200
1100
1000
900
800
700
600
500
400
300
200
Dec–11–99 00:00
Dec–16–99 00:00
Dec–21–99 00:00
Dec–26–99 00:00
Dec–31–99 00:00
Jan–05–00 00:00
time – (hours)

Figure 3

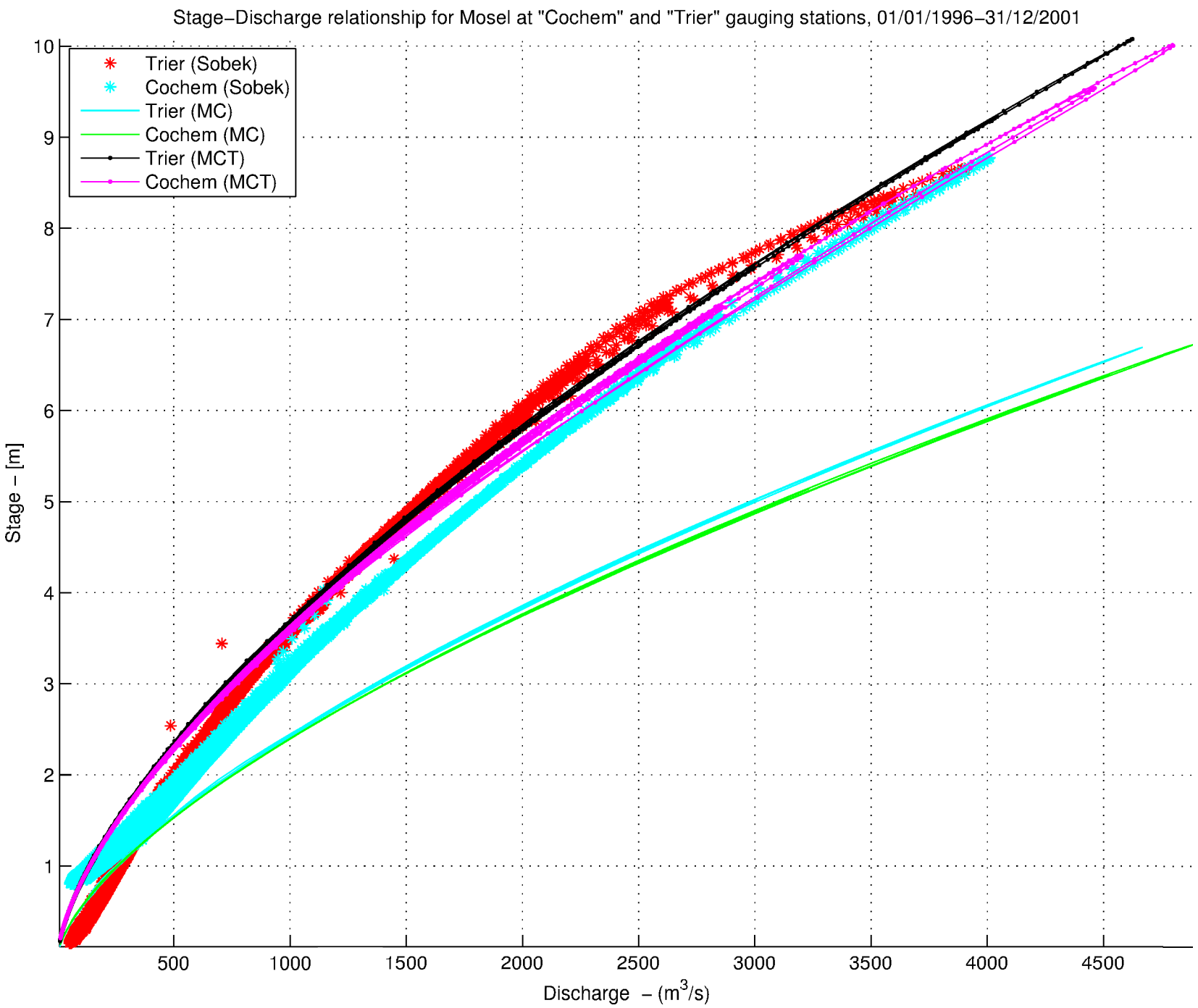
Stage–Discharge relationship for Mosel at "Cochem" and "Trier" gauging stations, 01/01/1996–31/12/2001
Trier (Sobek)
Cochem (Sobek)
Trier (MC)
Cochem (MC)
Trier (MCT)
Cochem (MCT)
Stage – [m]
Discharge – (m3/s)
1
2
3
4
5
6
7
8
9
10
500
1000
1500
2000
2500
3000
3500
4000
4500

Figure 4

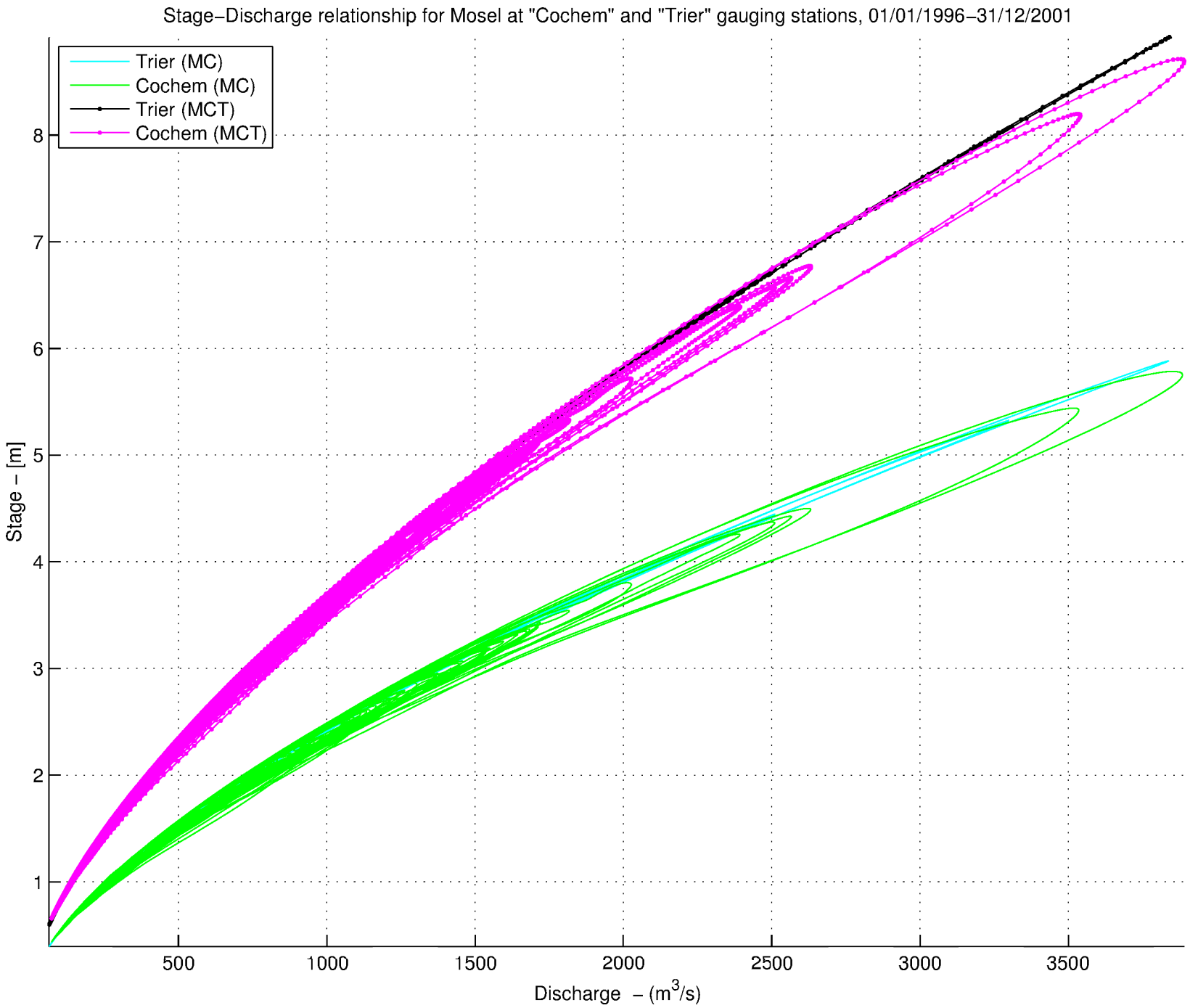
Stage–Discharge relationship for Mosel at "Cochem" and "Trier" gauging stations, 01/01/1996–31/12/2001
Trier (MC)
Cochem (MC)
Trier (MCT)
Cochem (MCT)
Stage – [m]
1
2
3
4
5
6
7
8
500
1000
1500
2000
2500
3000
3500
Discharge – (m3/s)

Figure 5